Efficient removal of Cu(II) from aqueous systems using Enhanced-quantum Yield Nitrogen doped Carbon Nanodots

Mohammed Abdullah Issa[1], Zurina Z. Abidin[1], Musa Y. Pudza[1], Hamid Zentou[1]

[1]Department of Chemical and Environmental Engineering, Faculty of Engineering, Universiti Putra Malaysia, 43400 UPM Serdang, Selangor, Malaysia

Supplementary data

Section I

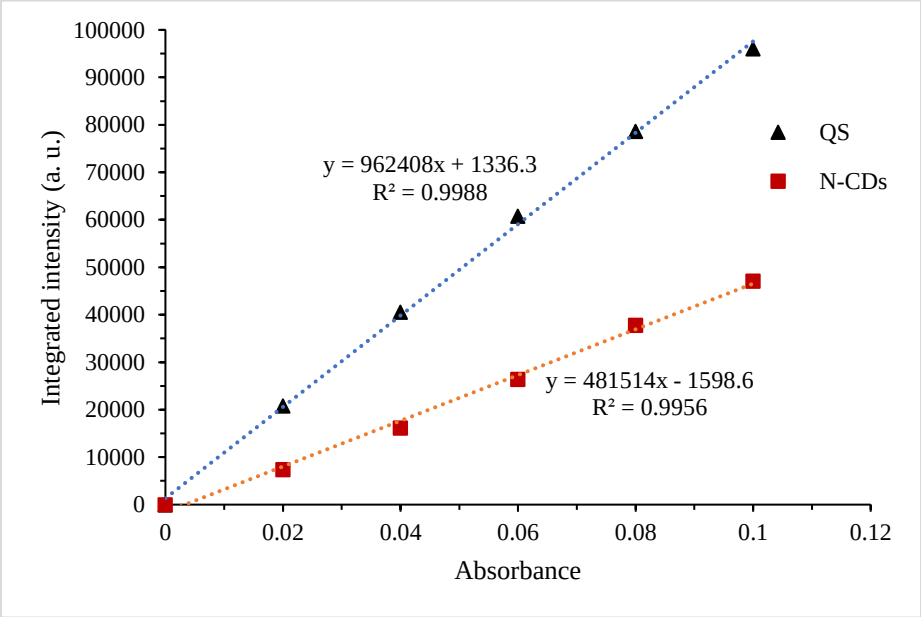

Figure S1. The relation between fluorescence integral intensity and absorbance (the slope of lines indicated the QY of N-CDs)

Table S1. Optimization of PEG concentration for the production of N-CDs

No.	Starting materials ratio		Quantum yield (QY)
	CMC	PEG weight	
1	0.2 g	0%	8
2	0.2 g	10%	14
3	0.2 g	20%	23
4	0.2 g	30%	18

Table S2. Optimization of synthesis conditions for the production of N-CDs

No.	Synthesis temperature	Reaction time	Quantum yield (QY)
1	230°C	6hr	16
2	250°C	6hr	23
3	270°C	6hr	27
4	260°C	1hr	20
6	260°C	3hr	22

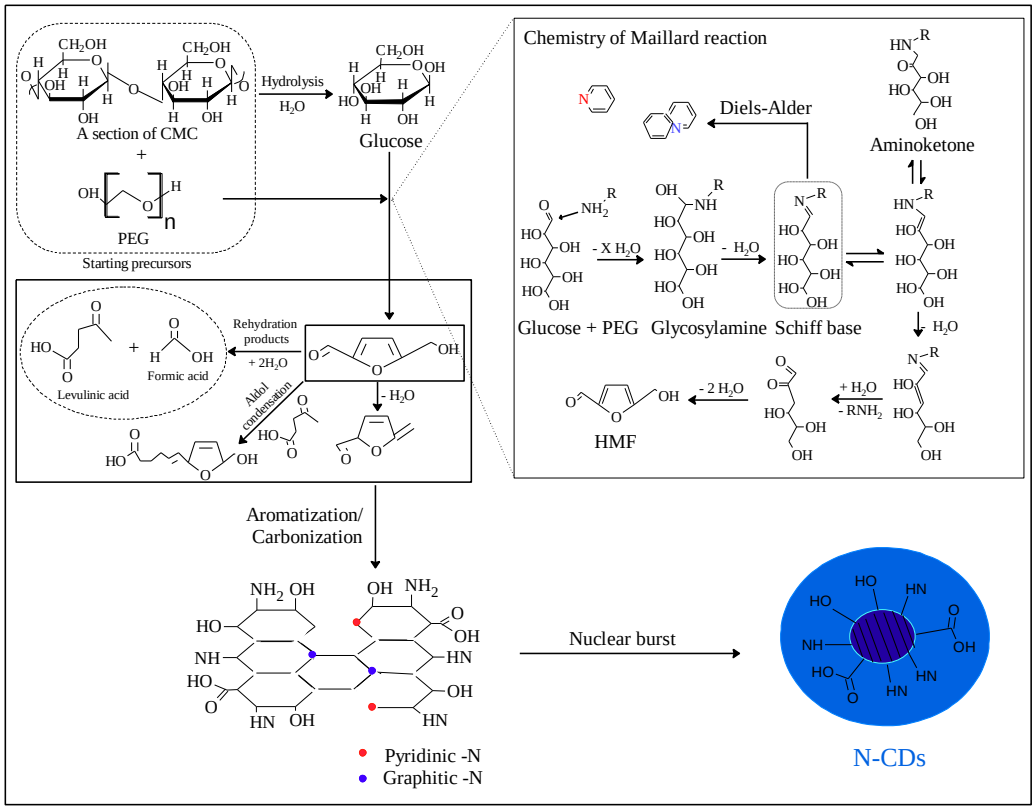

Figure S2. A proposed formation mechanism of N-CDs

Section II

Characterization of N-CDs

EDA analysis was used to gain insight into the elemental composition of the obtained nanodots. Compared to the undoped CDs, the EDS of N-CDs (Table S4) displays a noticeable N contents with an atomic ratio of 22.6%, indicating the successful nitrogen-passivation process. The rising of carbon weight along with the oxygen content reduction confirms the aromatization process with the elimination of O moieties.

Table S3. Elemental compositions of the undoped and N-CDs

Sample	C/atomic %	O/atomic%	N/atomic%
CDs	52.7	30.9	ND*
N-CDs	61.2	9.5	22.6

Note. ND: not detected.

FTIR spectra (Figure S2) confirms the presence of plenty functional groups on the edge of N-CDs. More specifically, the peak at 3374 cm^{-1} is ascribed to the stretching vibration of N-H/ O-H. The peaks at 2150 cm^{-1} and 765 cm^{-1} attributed to C-H stretching and bending mode, respectively whereas the peak at 1641 cm^{-1} is corresponded to C=O in the conjugated domain. The characteristic stretching band of the C=N and C-N bonds were observed at 1366 cm^{-1} and 1213 cm^{-1}. The formation of N-H, C=N and C-N moieties indicate the effective involvement of PEG into the final domain of N-CDs. The peaks at 1094 cm^{-1} and 960 cm^{-1} were related to C-O and C-O-C, demonstrating the oxidation of hydroxyl groups in the CMC molecule.

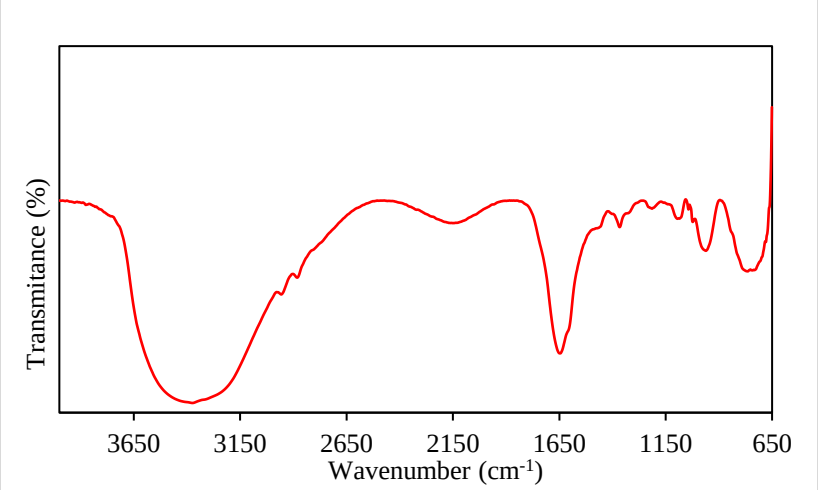

Figure S3. FTIR spectra of N-CDs

Further insight into the elemental composition and binding structure of N-CDs was recorded by XPS spectrum. As shown in Figure S3a, the wide XPS spectrum demonstrates that the obtained N-CDs are mainly composed of carbon, nitrogen, and oxygen. The narrow scan of C_1s (Figure S3b) presents four main peaks ascribed to the four states of carbon bonds (C-C, C-N, C-O and C=O). The N_1s scan (Figure S3c) confirm the presence of graphitic N, pyridinic N and N–H, suggesting that N has been successfully incorporated into the framework of N-CDs in different modes. The O_1s scan (Figure S3d) displays two peaks of O-H and C=O.

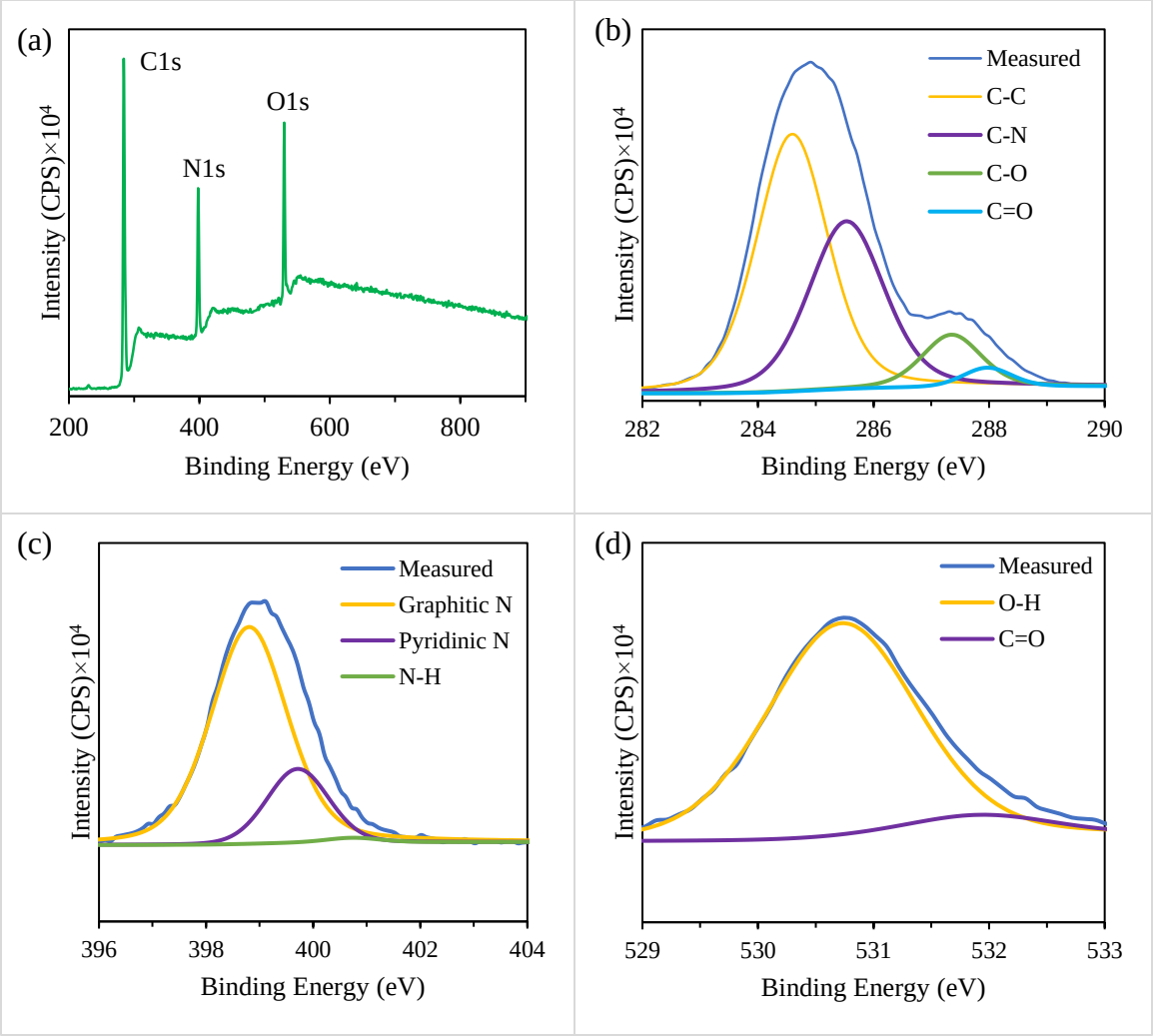

Figure S4. (a) XPS wide survey of N–CDs. The high-resolution XPS spectra of (b) C1s, (c) N1s and (d) O1s

Section III

Adsorption isotherm

To explain the performance of the N-CDs towards Cu(II), Langmuir and Freundlich models were used. Langmuir isotherm (Eq. S1) assumes that is no reduction with adsorbent sites whereas Freundlich (Eq. S2) proposes that there is an exponential decline of adsorption surface and energies [47]. In its linear plot, the Langmuir and Freundlich isotherm can be expressed as:

Langmuir model:

$$\frac{C_e}{q_e} = \frac{C_e}{q_m} + \frac{1}{q_m K_L} \quad \text{(S1)}$$

Freundlich model:

$$\log q_e = \log K_F + \frac{1}{n}(\log C_e) \quad \text{(S2)}$$

where q_e and C_e are adsorption capacity (mg/ g) and Cu(II) concentration (mg/L) in solution at equilibrium, respectively. q_m is the maximum adsorption capacity (mg/ g) and K_L is Langmuir constant. Freundlich variable K_F represents Freundlich adsorption uptake of the absorption experiment and *n* indicates the isotherm nonlinearity. A dimensionless factor (R_L), can be used to assess the feasibility of adsorption process expressed as:

$$R_L = \frac{1}{1+K_L C_o} \quad \text{(S3)}$$

where K_L is the Langmuir constant (L mg^{-1}) and C_o is the initial concentration (mg/L). The adsorption system is favorable if $0 < R_L < 1$, unfavorable if $R_L > 1$and linear if $R_L = 1$, irreversible if $R_L = 0$.

Reference

[1] S. Jayaweera, K. Yin, X. Hu, and W. J. Ng, "Facile preparation of fluorescent carbon dots for label-free detection of Fe3+," *J. Photochem. Photobiol. A Chem.*, vol. 370, no. October 2018, pp. 156–163, 2019.

[2] J. Wang *et al.*, "WITHDRAWN: One-pot simple green synthesis of water-soluble cleaner fluorescent carbon dots from cellulose and its sensitive detection of iron ion," *J. Clean. Prod.*, 2017.

[3] P. Shen, J. Gao, J. Cong, Z. Liu, C. Li, and J. Yao, "Synthesis of Cellulose-Based Carbon Dots for Bioimaging," *ChemistrySelect*, vol. 1, no. 7, pp. 1314–1317, 2016.

[4] Q. Wu, W. Li, J. Tan, Y. Wu, and S. Liu, "Hydrothermal carbonization of carboxymethylcellulose: One-pot preparation of conductive carbon microspheres and water-soluble fluorescent carbon nanodots," *Chem. Eng. J.*, vol. 266, pp. 112–120, 2015.

[5] M. Abdullah Issa *et al.*, "Fabrication, characterization and response surface method optimization for quantum efficiency of fluorescent nitrogen-doped carbon dots obtained from carboxymethylcellulose of oil palms empty fruit bunch," *Chinese J. Chem. Eng.*, 2019.

[6] P. Wu, W. Li, Q. Wu, Y. Liu, and S. Liu, "Hydrothermal synthesis of nitrogen-doped carbon quantum dots from microcrystalline cellulose for the detection of Fe 3+ ions in an acidic environment," *RSC Adv.*, vol. 7, no. 70, pp. 44144–44153, 2017.

[7] S. Jayaweera, K. Yin, X. Hu, and W. J. Ng, "Fluorescent N/Al Co-Doped Carbon Dots from Cellulose Biomass for Sensitive Detection of Manganese (VII)," *J. Fluoresc.*, 2019.

[8] G. Yang, X. Wan, Y. Su, X. Zeng, and J. Tang, “Acidophilic S-doped carbon quantum dots derived from cellulose fibers and their fluorescence sensing performance for metal ions in an extremely strong acid environment,” *J. Mater. Chem. A*, vol. 4, no. 33, pp. 12841–12849, 2016.

[9] N. Chaudhry, P. K. Gupta, S. Eremin, and P. R. Solanki, “One-step green approach to synthesize highly fluorescent carbon quantum dots from banana juice for selective detection of copper ions,” *J. Environ. Chem. Eng.*, vol. 8, no. 3, p. 103720, 2020.

[10] L. Adinarayana *et al.*, “Single Step Synthesis of Carbon Quantum Dots from Coconut Shell : Evaluation for Antioxidant Efficacy and Hemotoxicity,” *J. Mater. Sci. Appl.*, vol. 3, no. 6, pp. 83–93, 2017.

[11] J. Yu *et al.*, “Luminescence mechanism of carbon dots by tailoring functional groups for sensing Fe3+ ions,” *Nanomaterials*, vol. 8, no. 4, pp. 1–12, 2018.